Soft Matter

ARTICLE TYPE

Cite this: DOI: 10.1039/xxxxxxxxxx

Supplementary Information: Needle-Induced Cavitation of Cylindrical Voids

Christopher W. Barney,[a] Yue Zheng,[b] Shuai Wu,[b] Shengqiang Cai,[b] and Alfred J. Crosby,[*a]

Received Date
Accepted Date

DOI: 10.1039/xxxxxxxxxx

www.rsc.org/journalname

1 Experimental Variables Details

The following sections describe the exact experimental conditions and trials measured in this study.

1.1 Needle-Induced Cavitation With Retraction

Gel chemistries were tested across 7 vol.% $A_{25}B_{104}A_{25}$ gels injected with air and 30.7 PDMS blends (18 hour cure) injected with water with the majority of experimental parameters being tested on the $A_{25}B_{104}A_{25}$ gels due to their thermoreversible nature. $A_{25}B_{104}A_{25}$ gels were probed with needle size (R_{in}, R_{out})={(156,283),(130,232),(80,156)} μm, $\dot{\delta}$={0.1,1,10} mm/s, δ_{max}={16,22} mm, injection rate $\dot{V}$={50,500,2500} μL/min, and $d_{retraction}$={0,2,4,6,8} mm. The R_{in}=156 and 80 μm needles were only probed with $\dot{\delta}$=1 mm/s and a constant injection rate of 500 μL/min was used for all measurements except for the $\dot{\delta}$=1 mm/s, R_{in}=130 μm conditions which were also tested at the 50 and 2500 μL/min rates. Five trials were performed at each experimental condition totalling 350 trials on the $A_{25}B_{104}A_{25}$ gel. 30.7 PDMS blends were probed with needle size (R_{in}, R_{out})={(130,232)} μm, $\dot{\delta}$={0.1,1,10} mm/s, δ_{max}={10,22} mm, injection rate $\dot{V}$={50} μL/min, and $d_{retraction}$={0,2,4,6,8} mm. Five trials were performed at each experimental condition totalling 150 trials on the 30.7 PDMS blend. In total 100 experimental conditions were tested across 500 trials. Summary data is available in Supplementary Text File ST1.

1.2 Estimating Critical Retraction Distance

An experiment was conducted on the PDMS blends listed in Table 1 of the main text that were cured for 24 hours with (R_{in}, R_{out})=(130,232) μm, $\dot{\delta}$=0.1 mm/s, δ_{max}=22 mm, $\dot{V}$=50 μL/min, and $d_{retraction}$=10 mm. The 40.95 PDMS blend was also tested with (R_{in}, R_{out})={(156,283),(80,156)} μm. A total of 5 trials were performed for each experimental condition totaling 35 trials across 7 experimental conditions. Summary data is available in Supplementary Text File ST2.

References

[a] Polymer Science and Engineering Department, University of Massachusetts, 120 Governors Drive, Amherst, MA, 01003, USA. Fax: +1 413 545 0082; Tel: +1 423 577 1313; E-mail: crosby@mail.pse.umass.edu
[b] Department of Mechanical and Aerospace Engineering, University of California, San Diego, La Jolla, CA 92093, USA.

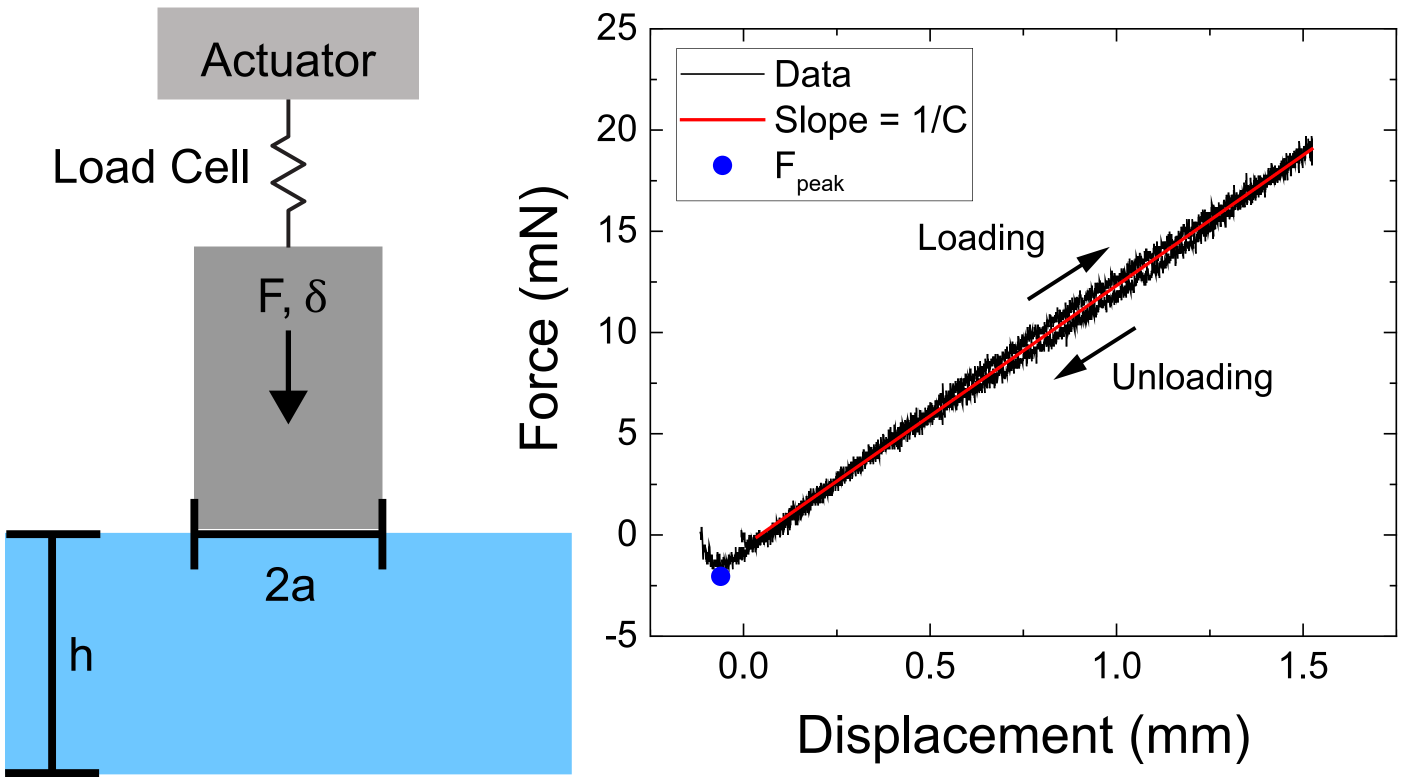

Fig. S1 Schematic of the setup used to measure the force F and displacement δ during indentation with a representative plot of force against displacement for the $A_{25}B_{104}A_{25}$ gel. Compression is positive F while tension is negative F. Displacement is zeroed at the contact point between the probe and the sample. Both the loading and unloading curves are shown on the plot and are nearly overlapping showing the highly elastic response of the $A_{25}B_{104}A_{25}$ gel. The slope of the data represents the observed stiffness, which is the inverse the observed compliance C, while the blue dot represents the peak separation force F_{peak} during unloading.

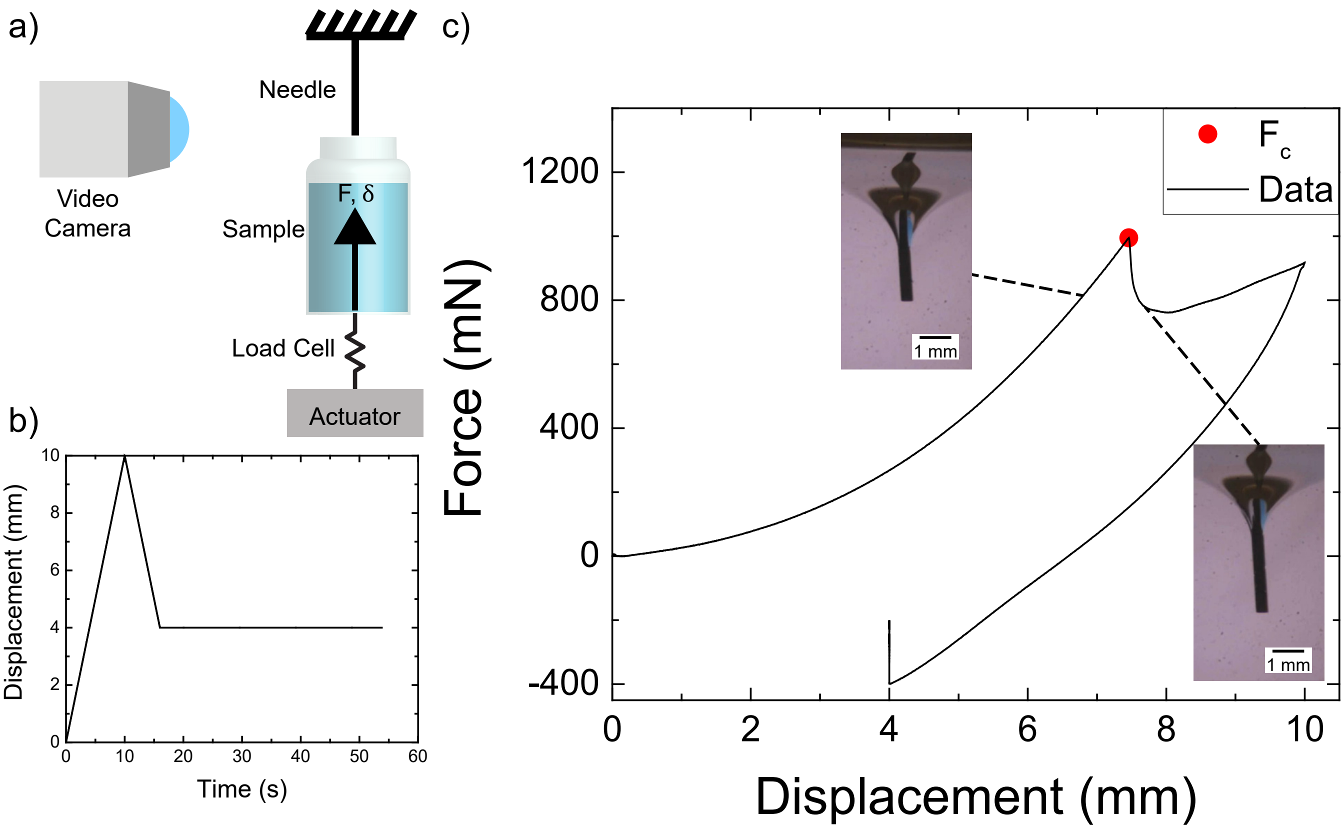

Fig. S2 a) Schematic of the setup used to measure the force, displacement, and video during puncture. b-c) Plot of displacement against time and force against displacement during the puncture test of a 30.7 PDMS blend. Positive force is compression while negative force is tension. The red dot represents the critical puncture force F_c. Images of the needle before and after F_c are shown on the force-displacement plot.

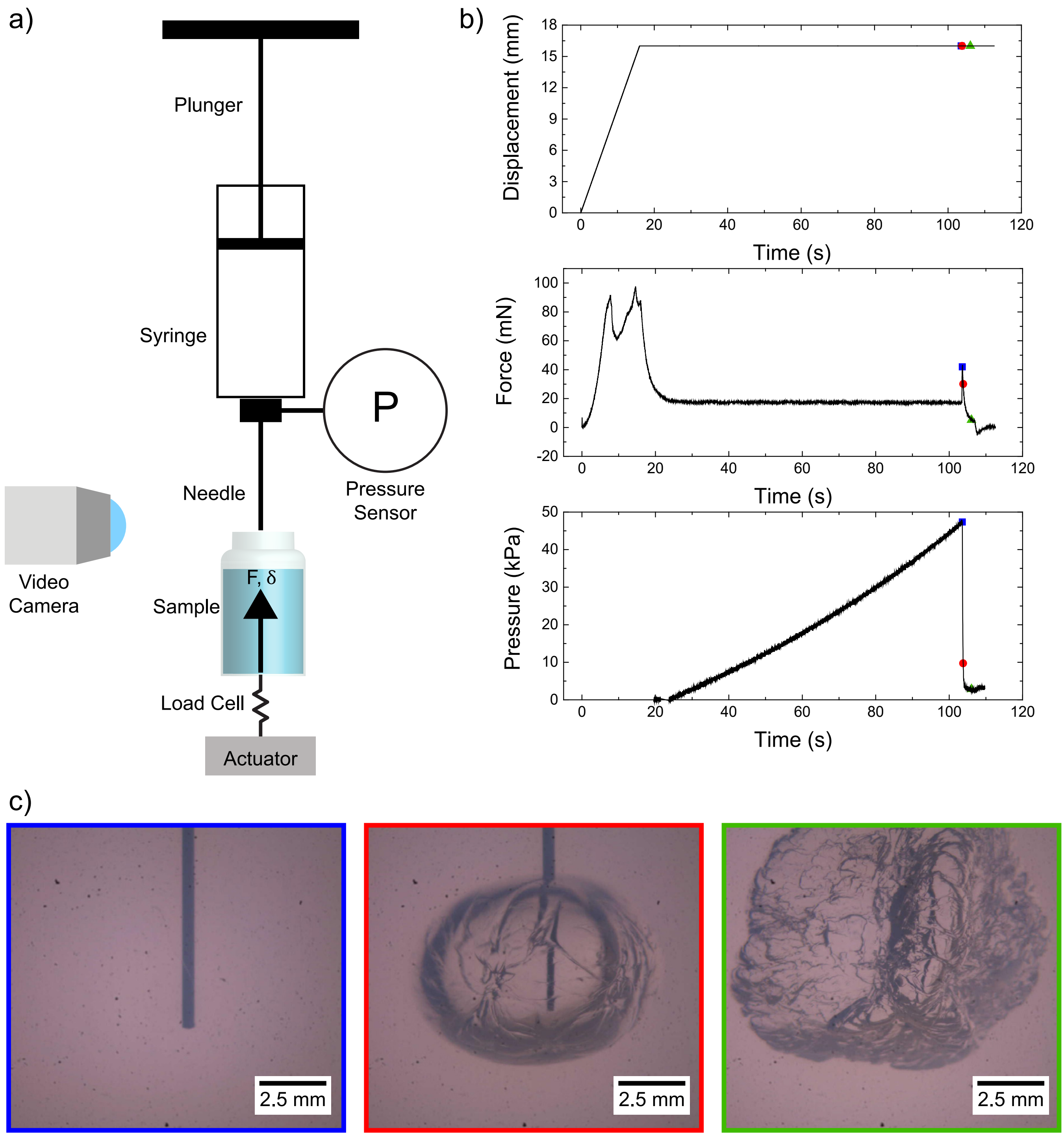

Fig. S3 a) Schematic of the setup used to measure the force and displacement of the needle, pressure at the needle tip, and video during needle-induced cavitation. b) Plots of displacement of the needle, force on the needle, and pressure at the needle tip against time for a representative run on the $A_{25}B_{104}A_{25}$ gel. c) Images corresponding to the blue, red, and greed data points in b). This is the same run shown in Supplementary Video SV1.

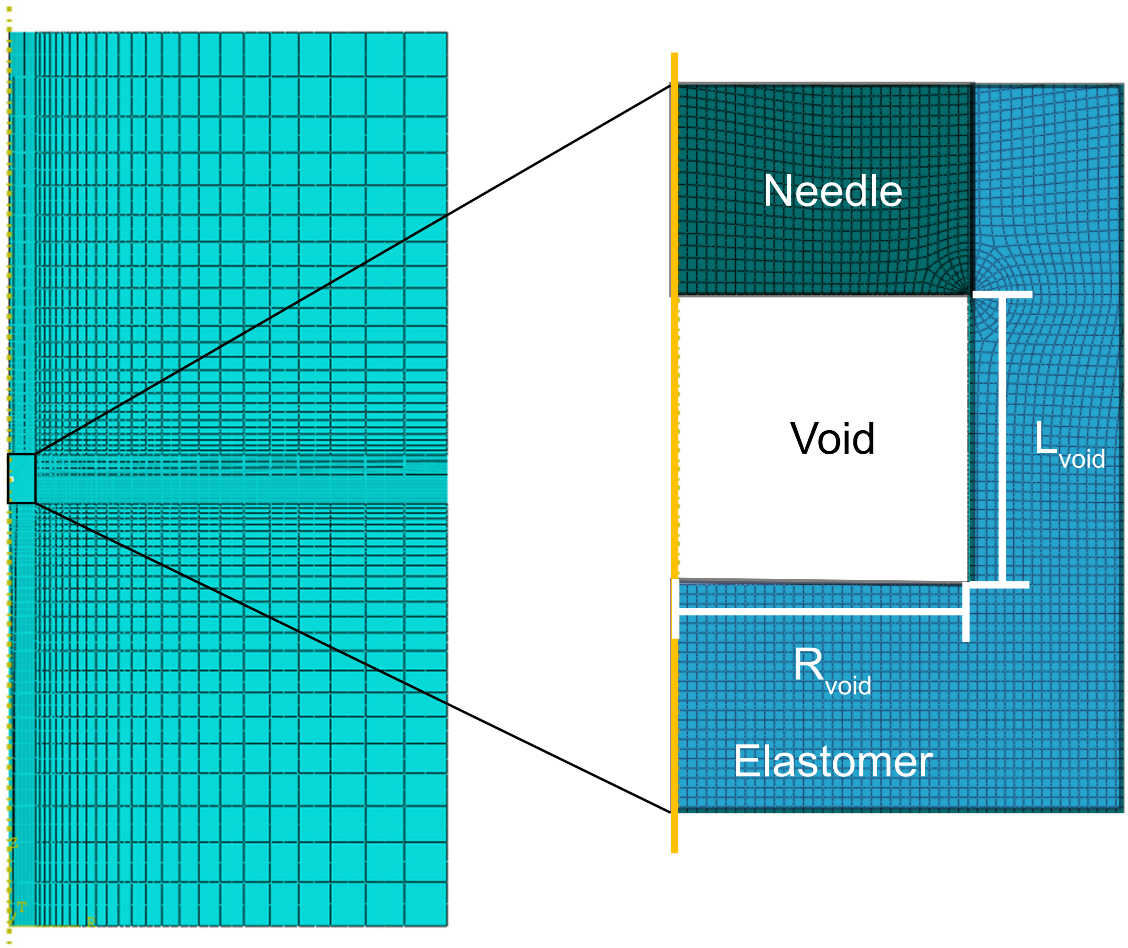

Fig. S4 Distribution of the nodes used in the finite element simulation. The density of nodes greatly increases near the void. Height and radius of the sample block are set to 100 and 50 times R_{void} respectively.

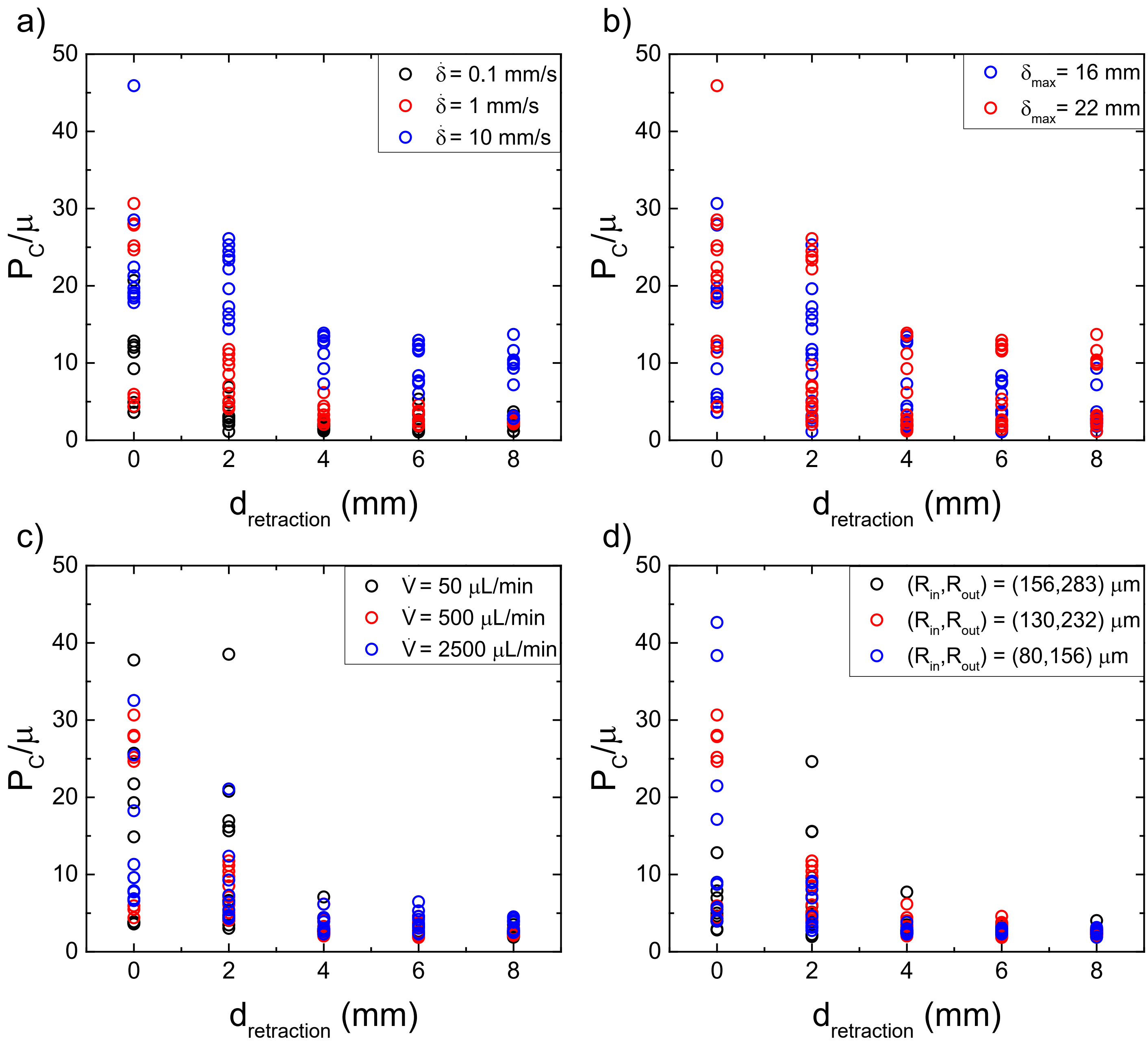

Fig. S5 Plots of P_c/μ for the $A_{25}B_{104}A_{25}$ gel showing the interaction between $d_{retraction}$ and a) $\dot{\delta}$, b) δ_{max}, c) $\dot{V}$, and d) (R_{in}, R_{out}). $\dot{\delta}$=10 mm/s appears to produce consistently higher pressures than the lower needle insertion speeds. A weak trend is observed where increasing $\dot{V}$ increases P_c at larger $d_{retraction}$. Beyond that and the previously discussed dependence on $d_{retraction}$ no other trends are apparent in the data.

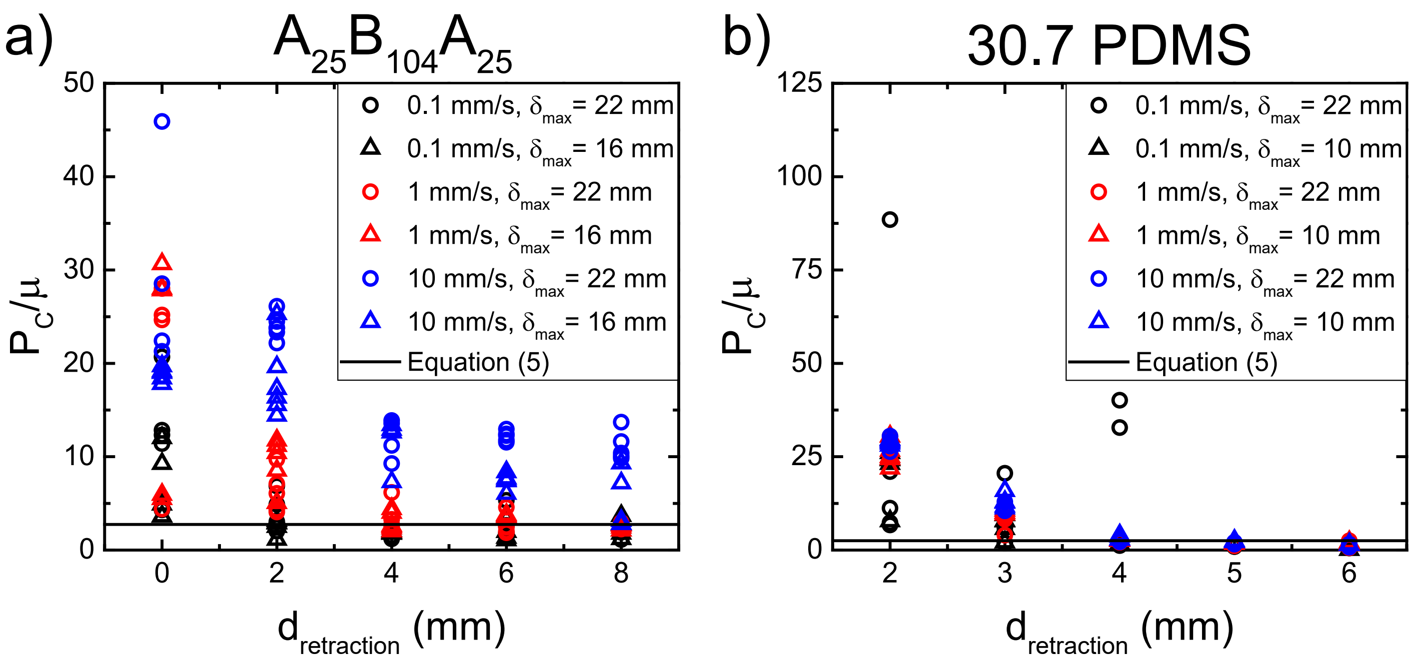

Fig. S6 Plots of critical pressure P_c normalized by the shear modulus μ against $d_{retract}$ for the a) $A_{25}B_{104}A_{25}$ gel and b) 30.7 PDMS blend where (R_{in}, R_{out})=(130,232) μm and $\dot{V}$=500 μL/min in the $A_{25}B_{104}A_{25}$ gel and $\dot{V}$=50 μL/min in the 30.7 PDMS blend. At small $d_{retraction}$ large pressures with high variability for each gel is observed.

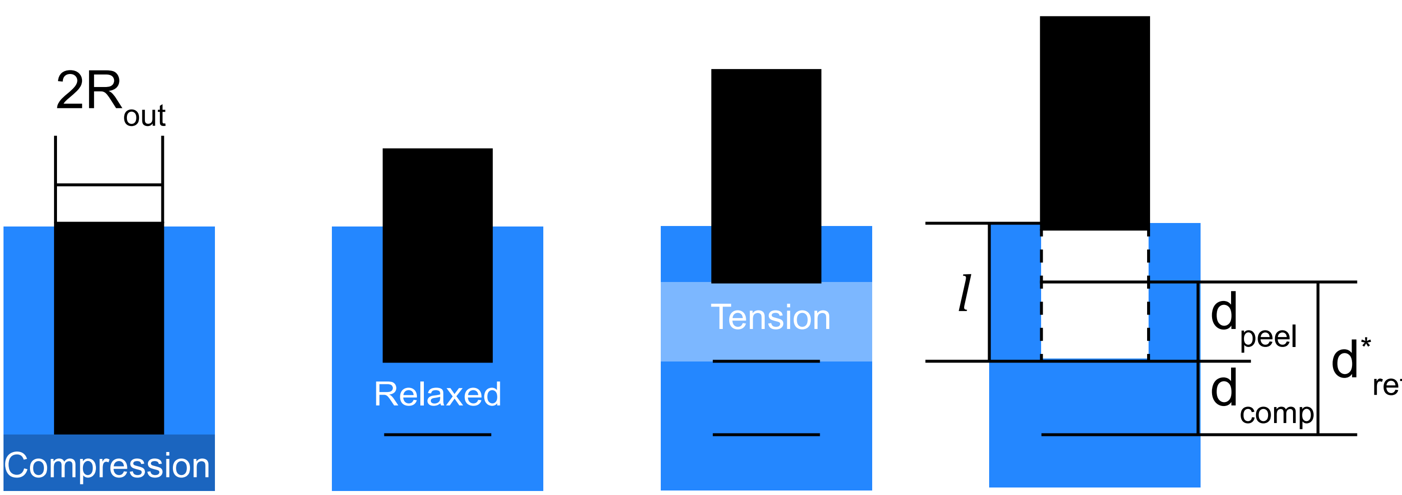

Fig. S7 Schematic of the retraction process. Starting at δ_{max}, compressive strains are imposed below the needle through direct transfer of stress across the interface between the needle tip and gel. Upon retraction, these compressive strains relax and a tension is induced. Finally, a critical amount of tensile energy is stored to overcome the strength of the interface and the needle tip goes from a contacting to a non-contacting state at $d_{retraction} > d^*_{ret}$. Note that residual strains will also be present at the walls between the needle and gel. However, pressure is applied directly down from the needle tip so the compressive strains below the needle have the most impact on critical pressures.